

# PredictionNet: Real-Time Joint Probabilistic Traffic Prediction for Planning, Control, and Simulation

Alexey Kamenev, Lirui Wang, Ollin Boer Bohan, Ishwar Kulkarni, Bilal Kartal  
Artem Molchanov, Stan Birchfield, David Nistér, Nikolai Smolyanskiy

NVIDIA

**Abstract**—Predicting the future motion of traffic agents is crucial for safe and efficient autonomous driving. To this end, we present PredictionNet, a deep neural network (DNN) that predicts the motion of all surrounding traffic agents together with the ego-vehicle’s motion. All predictions are probabilistic and are represented in a simple top-down rasterization that allows an arbitrary number of agents. Conditioned on a multi-layer map with lane information, the network outputs future positions, velocities, and backtrace vectors jointly for all agents including the ego-vehicle in a single pass. Trajectories are then extracted from the output. The network can be used to simulate realistic traffic, and it produces competitive results on popular benchmarks. More importantly, it has been used to successfully control a real-world vehicle for hundreds of kilometers, by combining it with a motion planning/control subsystem. The network runs faster than real-time on an embedded GPU, and the system shows good generalization (across sensory modalities and locations) due to the choice of input representation. Furthermore, we demonstrate that by extending the DNN with reinforcement learning (RL), it can better handle rare or unsafe events like aggressive maneuvers and crashes.

## I. INTRODUCTION

Safe and effective autonomous driving requires accurately predicting the motion of nearby actors, such as vehicles, pedestrians, and cyclists. An autonomous vehicle needs to anticipate whether a nearby car will keep moving forward at constant speed, brake suddenly, or cut into an adjacent lane. Predicting other agents’ behaviors has been shown beneficial both in adversarial and cooperative domains [1], [2].

Brute-force enumeration of all possible actions leads to combinatorial explosion, creating a computational bottleneck. Similarly, most recent approaches [3], [4], [5], [6], [7], [8] use very deep networks (e.g., ResNet50), predict each agent separately or use batches of cropped feature maps, which precludes real-time operation. We seek a system that jointly predicts the motions of all actors, is not limited to the number of actors, is agnostic to input sensory modality, runs in real-time, and handles rare/unsafe events.

In this paper, we propose a novel system which, to our knowledge, is the first to satisfy these requirements. Our system, called PredictionNet, relies on a simple yet flexible representation for both input and output. The current state (input) is a top-down multi-layer rasterization of the perceived vehicle boundaries and relevant scene context provided by the map’s lane dividers. The method is agnostic to the perception modality as it relies on its own representation

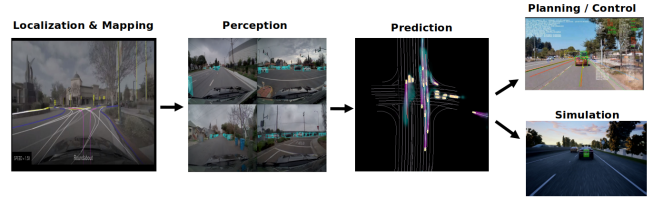


Fig. 1: Simplified autonomous driving diagram. PredictionNet can be used for planning / control, or simulation.

created by top-down rasterization. The predicted state (output) is a top-down representation providing the probability density function (PDF) of all traffic actors’ future poses along with estimated velocities and backtrace vectors to aid trajectory extraction. The system is trained on real driving data to simultaneously predict full PDFs of the motion of all observed traffic agents and the ego-vehicle in a single pass. The network can be used for both realistic simulation and closed-loop planning/control (Fig. 1).

We have incorporated PredictionNet into the closed-loop planning/control stack of a real-world autonomous driving system. The network runs *faster than real-time*, providing sufficient time for the planner to react safely.<sup>1</sup> The network effectively predicts on camera and radar derived data, despite training only on LiDAR data. We show improvements in real driving behavior compared to an analytical baseline, as well as competitive offline results on both the INTERACTION prediction benchmark [9] and an internal dataset.

The learned network can also be used for real-time traffic simulation. As such, it avoids the common problems of simulators that rely on hand-coded rules and replay from driving logs. The former cannot capture complex interactions, while the latter cannot be used to study rare or unsafe behaviors, because datasets collected from actual drives necessarily under-represent such events. We use this simulator, together with reinforcement learning (RL), to extend our network with an ego-policy head that encourages collision-free driving beyond the expert dataset distribution.

Our contributions are as follows:

- A network that predicts all traffic agents, including the ego-vehicle, and models their interactions in one pass;

<sup>1</sup>Our system requires **5 ms** for inference plus **3 ms** for pre-/post-processing, on an embedded NVIDIA Drive AGX platform. By comparison, our closest competitor MultiPath [5] is an order of magnitude slower.

- Flexible probabilistic output representation that allows modeling of an arbitrary number of traffic agents;
- Faster than real-time performance, and agnostic to input sensory modalities (LiDAR / radar / camera);
- A model-based reinforcement learning extension to handle rare or unsafe events.

## II. PREVIOUS WORK

**Traffic Prediction.** A number of analytical and deep learning approaches to vehicle prediction have been proposed. Analytical methods typically use heuristics such as lane following with constant velocity. Despite the stability of classical prediction methods, deep neural networks (DNN) often provide better predictions across diverse traffic scenarios. Specifically, DESIRE [3] uses a conditional variational auto-encoder (CVAE [10]) to obtain future prediction samples, then uses an RNN-based scoring module for ranking. A top-down LiDAR scan is encoded via a convolutional neural network (CNN) to provide a scene context. With similar encodings for map and observations, PRECOG [4] employs a probabilistic model of future interactions between agents, conditioned on the goal of the ego-actor. MultiPath [5] uses a set of anchors for trajectory prediction. Each anchor corresponds to a mode in the trajectory distribution and together they form a Gaussian mixture model. VectorNet [11] relies on vectorization of map lanes and past trajectories via a graph neural network (GNN [12]) and uses attention mechanism for predicting. MultiXNet [6] provides object detection jointly with trajectory prediction from LiDAR input. The prediction stage uses a batch of cropped top-down feature maps encoded by the detector stage to produce multi-modal predictions. ILVM [7] defines the distribution over future trajectories by using implicit latent variable model. The system uses a CNN to encode scene context, crops its feature maps for each actor and then uses GNN for latent learning and prediction. Trajectron++ [8] jointly learns to predict controls for all agents with a GNN and then integrates agent trajectories using vehicle-dynamics models. Most DNN-based approaches predict behavior for each traffic agent separately and only predict behavior for non-ego agents. Therefore, they cannot be used for ego-motion planning directly and/or would be too slow for real-time applications.

**Traffic Simulation.** Simulation is a safe and controllable way to evaluate system performance against diverse scenarios. Rule-based simulators such as CARLA [13] and SUMO [14] are widely used in benchmarks and tests. However, policies learned in these simulators often transfer poorly to reality due to lack of realistic behaviors. Several recent works [15], [16] have been proposed to simulate traffic in a data-driven fashion. TrafficSim [15] uses a graph neural network and a generative model to synthesize rare traffic scenarios. However, the model runs at 0.5 frames per second (FPS) and is therefore hard to deploy in real-time driving. SimNet [16] trains a single-step action model for realistic simulation, to evaluate performance of motion planners.

**Planning and Control.** There is a large body of literature on the use of traffic predictions for online planning and of

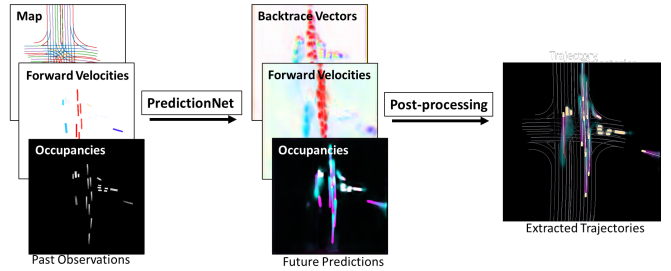


Fig. 2: Pipeline diagram. The velocities and vectors are shown using a standard optical flow color map, while the occupancy and trajectory visualizations transition from magenta to cyan in time. The yellow boxes in the far right image show the current vehicles.

fine policy learning. Analytical traffic forecasting and hand-coded cost functions [17], [18] are widely used to satisfy constraints such as traffic rules and collision avoidance. On the other hand, learning-based planning methods [19]–[21] have shown progress on reactive behavior and generalization in complex driving scenarios. Many works [22]–[25] use imitation learning (IL) to mimic demonstrated traffic behavior. The simplest example is behavior cloning (BC) that suffers from the known distribution-shift problem [26]. Another paradigm is reinforcement learning (RL). Due to the high-dimensional inputs and sparse rewards, model-free RL [27]–[32] approaches are sample inefficient, rendering them impractical for real-world driving. Using model-based RL with learned traffic models allows us to train realistic policies that can learn to react to rare/unsafe events injected in a simulator.

## III. METHOD

### A. PredictionNet

1) *Data representation:* Our approach to traffic prediction relies upon a single deep neural network to transform the current traffic scene input into predicted future motion for all traffic agents, including the ego-vehicle; and a post-processing step to extract trajectories (Fig. 2). The traffic scene, which is rasterized in a top-down view, is perceived by a separate system (using camera, radar, and/or LiDAR) to include data for all traffic agents surrounding the ego-vehicle along with the current map (e.g., lane dividers). This approach allows the network to predict the motion of an arbitrary number of traffic agents without any extra compute.

Let  $M_t \in \mathbb{R}^{2 \times h \times w}$  be a rasterized representation of the road geometry, transformed into the ego-vehicle's frame of reference at the time  $t$  of prediction. The ego-vehicle is at the center, oriented to point upward. Each entry in  $M_t$  indicates one of a discrete number of road line types, depending upon the travel direction allowed, or zero if there is no road line at that pixel; the second channel stores the altitude of each lane divider relative to the ego-vehicle. Similarly, let  $O_t \in \mathbb{R}^{h \times w}$  be a binary image indicating the occupancy map of vehicles, where the vehicles are rendered as oriented rectangles.

Let  $V_t \in \mathbb{R}^{2 \times h \times w}$  represent the rasterized 2D forward velocities of those vehicles on the ground plane. Note that  $O_t = 0$  implies  $V_t = 0$ , since only the pixels corresponding

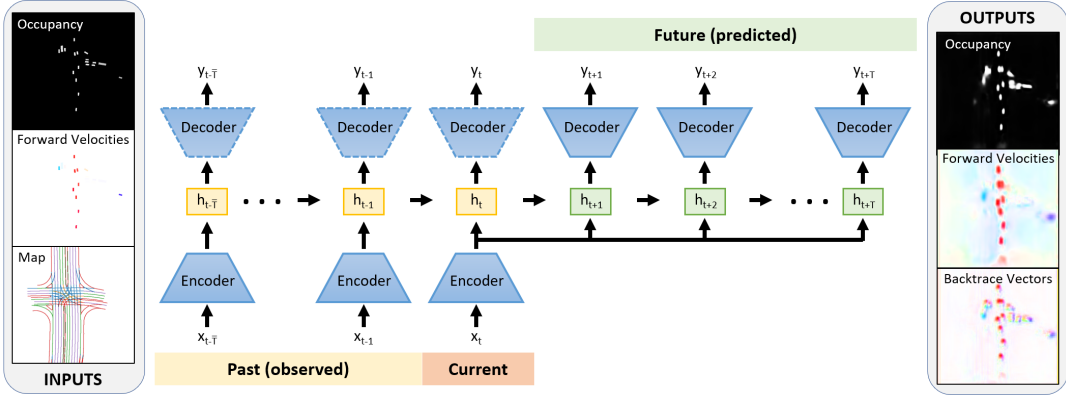


Fig. 3: Network diagram. Our network is a CNN encoder-decoder with two recursive neural network (RNN) models—one for processing past observations, and another for predicting the future. The past RNN (yellow) summarizes the observed velocities and occupancy along with the map. The latent state is then rolled out together with the current encoded input by the future RNN (green) to estimate future velocities and occupancy, along with backtrace vectors. The resulting sequence of future frames is used to extract the trajectories of all vehicles. The past decoders (dashed) are only used for training.

vehicles have non-zero velocities. For notational simplicity, let us treat  $t$  as an index. The dynamic inputs  $O_{t-\bar{T}+1:t}$  and  $V_{t-\bar{T}+1:t}$  for the past  $\bar{T}$  frames are stacked into a tensor  $x_t^{\text{dynamic}} \in \mathbb{R}^{\bar{T} \times 3 \times h \times w}$ , where the 3 channels arise from stacking the single-channel occupancy with the two-channel velocity images. The static input is simply  $x_t^{\text{static}} = M_t \in \mathbb{R}^{1 \times 2 \times h \times w}$ , where the 2 channels represent the type and altitude of nearby lane dividers. The input to the network at time  $t$  is the state  $x_t = (x_t^{\text{static}}, x_t^{\text{dynamic}})$ . The input tensor for each timestep is processed by an identical encoder.

The output is  $y_t = (\hat{O}_{t+1}, \hat{V}_{t+1}, \hat{W}_{t+1})$ , where  $\hat{O}_{t+1} \in \mathbb{R}^{h \times w}$  is the predicted occupancy map for the next time step,  $\hat{V}_{t+1} \in \mathbb{R}^{2 \times h \times w}$  contains the rasterized predicted forward velocities, and  $\hat{W}_{t+1} \in \mathbb{R}^{2 \times h \times w}$  contains additional backtrace vectors used to recover trajectories. A pixel in  $\hat{V}_{t+1}$  specifies the predicted *tangential* forward velocity from  $t$  to  $t+1$  in meters per second. A pixel in  $\hat{W}_{t+1}$  specifies the estimated vector from that pixel's location at  $t+1$  to the *center* of the corresponding vehicle at the previous time  $t$ . ( $\hat{W}$  captures the actual path, not the tangential motion.)

2) *Network Architecture and Training*: To summarize the past observations and predict into the future with a single forward pass, the network architecture is a simple 2D CNN encoder-decoder with two RNNs: one for processing past inputs, and another for predicting the future (Fig. 3). The inputs are represented as images and are encoded with CNNs into a latent space, which is shared by both RNN sequence models. For past observations up to the current time  $t$ , the internal past RNN state  $h_{t-k-1}$  is updated to  $h_{t-k}$  using  $x_{t-k}$ , where  $k = 0, \dots, \bar{T} - 1$ , and  $\bar{T}$  is the history buffer length. Given that  $h_t$  summarizes past observations, it can also be used for future predictions. Thus, for timesteps  $t+k$  after the current time-step, since we do not have full observations, we provide  $x_t$  as context and update  $h_{t+k}$  iteratively for  $k = 1, \dots, T$  up to the maximum horizon  $t+T$ . The future prediction is unrolled in an open-loop fashion where only the RNN hidden states are passed

between time-steps.

The network is trained end-to-end with supervised learning, where the latent state  $h_{t+k}$  at each time-step is decoded into  $y_{t+k}$ . We use a combination of focal loss [33] for the occupancy and  $L_2$  loss for the predicted backtrace vectors as well as velocities:

$$L(y_t) = L_{\text{focal}}(O_{t+1}, \hat{O}_{t+1}) + \lambda_1 \left\| V_{t+1} - \hat{V}_{t+1} \right\|_2^2 + \lambda_2 \left\| W_{t+1} - \hat{W}_{t+1} \right\|_2^2, \quad (1)$$

where  $\lambda_1, \lambda_2$  are scalar loss weights.

3) *Post-processing*: Trajectory extraction for all vehicles including the ego-vehicle is done via post-processing of the output tensors  $\{y_t, y_{t+1}, \dots, y_{t+T}\}$ . We start each trajectory at the initial position and velocity  $(p_t, v_t)$  given by the perception system. We roll out subsequent positions and velocities  $(p_{t+k}, v_{t+k})$  by integrating over the predicted velocity tensor, using the predicted occupancy tensor as a confidence signal, and using the backtrace vectors for drift-correction. This roll-out uses the following recurrence:

$$p_{t+1} = p_t + v_t \Delta t \quad (2)$$

$$\alpha = \sigma(w_\alpha \cdot \hat{O}_{t+1}[p_{t+1}] + b_\alpha) \quad (3)$$

$$p_{t+1} = p_{t+1} + \alpha \cdot \text{corr}_p(\hat{V}_t[p_{t+1}], \hat{W}_t[p_{t+1}]) \quad (4)$$

$$v'_{t+1} = \hat{V}_t[p_{t+1}] + \alpha \cdot \text{corr}_v(\hat{V}_t[p_{t+1}], \hat{W}_t[p_{t+1}]) \quad (5)$$

$$v_{t+1} = \alpha \cdot v'_{t+1} + (1 - \alpha) \cdot v_t \quad (6)$$

where  $\sigma$  is the logistic sigmoid function; and  $w_\alpha, b_\alpha \in \mathbb{R}$ ,  $\text{corr}_p, \text{corr}_v \in \mathbb{R}^{2 \times 4}$  are parameters set empirically (after PredictionNet training has completed) to minimize average displacement error (ADE) on the training set.

## B. PredictionNet for Closed-loop Traffic Simulation

After training on real-world data, PredictionNet can be used as a traffic simulation model. We initialize the state of the episodes with real data. Closed-loop roll-outs, using

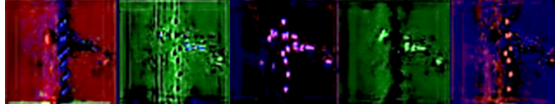


Fig. 4: Samples of latent vectors in PredictionNet. The latent space captures past agent interactions and map geometry.

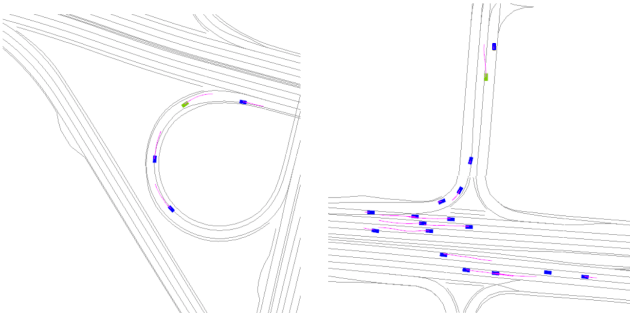


Fig. 5: Traffic simulations of PredictionNet. Green rectangle denotes the ego vehicle, blue rectangles are other actors, and magenta lines denote predictions. PredictionNet is able to generate realistic traffic under incomplete maps with varying topology.

the network as a stepping function, then simulate traffic offline. In this way, the network acts as a learned state-transition dynamics function that can be used to test planners in simulation and learn policies via reinforcement learning (RL).

We use the RNN’s latent encoding at the current time as a proxy for the state  $s_t = h_t$ . This latent state encodes the traffic history and lane geometry (Fig. 4). Let  $q_t$  be the configuration of the system, i.e., the positions and velocities of all actors. Given the current action  $a_t$ , we rasterize  $q_t$  and  $a_t$  into the input  $x_t$ , i.e. then encoded into the latent state  $s_t$ . We then rollout PredictionNet, and use post-processing to fit a unicycle kinematic model [34] to the decoder output  $y_{t+1}$ . This yields the configuration  $q_{t+1}$  to forward the simulation and close the loop with the updated history. Some examples are shown in Fig. 5. Note that whereas most systems provide only single-agent predictions, our DNN provides simultaneous multi-agent predictions conditioned on the ego-vehicle actions and other vehicles behaviors.

### C. Extending PredictionNet via Reinforcement Learning

Since PredictionNet is trained with supervised learning, it can be seen as a type of imitation learning. One drawback of imitation learning is its inability to handle rare/unsafe events that are not properly captured in the training data, such as cut-ins and harsh braking that might lead to collisions. To address these issues, we use a model-based RL framework and formulate the driving problem as an MDP with PredictionNet as the transition model. We train an additional policy head to produce ego actions, and we call this extension *PredictionNet-RL*.

In this work, we focus primarily on avoiding cut-ins and collisions caused by harsh braking, both of which are challenges for traditional adaptive cruise control (ACC). Each episode consists of three cars: a lead car, a neighbor car,

TABLE I: Network architecture, with  $\bar{T} = 6$  and  $T = 18$ . Time-steps are separated by 166.7 ms.

Layer description		Input	Output dimensions
0a	Input image (dynamic)	-	$6 \times 3 \times 512 \times 512$
0b	Input image (static)	-	$1 \times 2 \times 512 \times 512$
<b>Encoder:</b>			
1	2D convolution, ReLU	0a	$6 \times 16 \times 256 \times 256$
2	2D convolution, ReLU	0b	$1 \times 16 \times 256 \times 256$
2a	Add	1,2	$6 \times 16 \times 256 \times 256$
3	ResNet block	2a	$6 \times 32 \times 128 \times 128$
4	ResNet block	3	$6 \times 64 \times 64 \times 64$
5	ResNet block	4	$6 \times 64 \times 64 \times 64$
<b>RNN (past):</b>			
6-11	2D conv RNN, ASPPBlock [35], ReLU	5	$64 \times 64 \times 64$
<b>RNN (future):</b>			
12-29	2D conv RNN, ASPPBlock [35], ReLU	11	$64 \times 64 \times 64$
<b>Decoder:</b>			
30	Transposed ResNet block	29	$24 \times 64 \times 64 \times 64$
31	Transposed ResNet block	30	$24 \times 32 \times 64 \times 64$
32	Transposed ResNet block	31	$24 \times 16 \times 64 \times 64$
33	Upsample via 2D convolution	32	$24 \times 5 \times 128 \times 128$
34	Upsample (only training)	33	$24 \times 5 \times 512 \times 512$

and the ego car. Initial states are randomized. Non-ego cars are controlled by the PredictionNet prediction head, while the ego car is controlled by the RL policy head. In the cut-in task, the neighbor car executes a cut-in move when it observes a gap between the lead car and the ego car. In the collision-avoidance task, the lead car executes a random harsh braking event.

Our goal is to learn a policy  $\pi : s_t \mapsto a_t$  that maps the state  $s_t$  at time  $t$  to an action  $a_t$ , which is the ego vehicle’s acceleration. The task reward is defined as  $r_{\text{acc}} + r_{\text{rare}}$  where  $r_{\text{acc}}$  is a sum of manually designed reward terms such as distance to the lead car, acceleration changes, *etc.*, and  $r_{\text{rare}}$  is a sparse penalty term accounting for the rare events such as cut-ins and collisions. The trained RL policy learns to plan ahead, to reduce the gap and avoid cut-ins, and to keep a slower speed and avoid future harsh braking.

## IV. EXPERIMENTS

We investigate the following questions: (1) How well does PredictionNet perform on trajectory prediction benchmarks and internal datasets? (2) Can PredictionNet be used in a real-world actuated drive, and how does it compare to classical prediction methods? (3) Can we achieve feasible and reactive traffic simulation with PredictionNet? (4) Can we use PredictionNet-RL to improve ego vehicle behavior when encountering rare events?

### A. PredictionNet Performance

We summarize the detailed network architecture in Table I. The network is trained on  $512 \times 512$  images as inputs and outputs with 0.33 meter resolution per pixel thus providing  $170 \times 170$  m top-down field of view (FoV). The latent space is  $64 \times 64 \times 64$ . The focal loss scalar weight is set to 0.05, and other losses use  $\lambda_1 = \lambda_2 = 1.0$ . We compare our system with an analytical prediction baseline that utilizes kinematic models, assuming constant velocities and lane following. We use the following metrics to measure the prediction accuracy: Average Displacement Error (ADE) between corresponding points on predicted and ground truth trajectories, and Final Displacement Error (FDE) computed using only the final positions. Both are in meters.

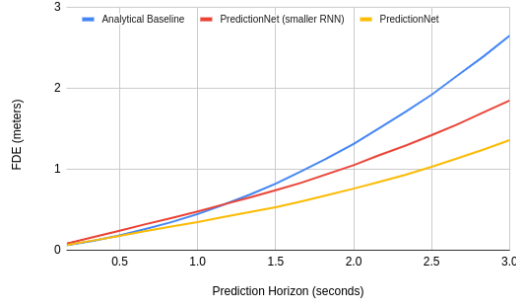


Fig. 6: FDE performances on internal dataset across horizons.

TABLE II: Comparison on INTERACTION dataset [9]. Results were taken from INTERPRET Challenge, NEURIPS20 stage, at 3 seconds prediction horizon. See text for details.

Model	Metric	set	1-traj	RT	ADE ( $\downarrow$ )	FDE ( $\downarrow$ )
DESIRE [3]		V	<span style="color:red">X</span>	<span style="color:red">X</span>	0.32	0.88
MultiPath [5]		V	<span style="color:red">X</span>	<span style="color:red">X</span>	0.30	0.99
TNT [36]		V	<span style="color:red">X</span>	<span style="color:red">X</span>	0.21	0.67
ReCoG [37]		V	<span style="color:red">X</span>	<span style="color:red">X</span>	0.192	0.646
ITRA [38]		V	<span style="color:red">X</span>	<span style="color:red">X</span>	0.17	0.49
PredictionNet (ours)		V	<span style="color:green">✓</span>	<span style="color:green">✓</span>	0.458	1.030
PredictionNet (ours)		R	<span style="color:green">✓</span>	<span style="color:green">✓</span>	0.518	1.228
SimNet [16]		G	<span style="color:red">X</span>	<span style="color:red">X</span>	0.652	1.670
MIFNet		G	<span style="color:red">X</span>	<span style="color:red">X</span>	0.534	1.425

PredictionNet achieves competitive results on the INTERACTION dataset [9], see Table II. We ran our network on both the validation (V) set and the “regular” test set (R). The “generalizability” test set (G) was not available at the time of submission. All published networks are listed. While it is difficult to compare across dataset versions, we would like to stress that our network has demonstrated generalization across locations and sensor modalities in real-world driving. As a result, we believe it is fair to compare our results with those on the generalizability (G) set, where our method is competitive. Note that our system is the only one that is evaluated using a single trajectory (most other systems produce 6 and measure the ADE/FDE of the best one), and ours is the only one that runs in real-time (RT).

We also achieve good results on a large internal driving dataset produced from LiDAR perception data, see Table III. The dataset is a mix of freeway and urban scenarios with both light and heavy traffic, containing more than 5000 km. Our approach outperforms an analytical baseline that relies on lane following and constant speed heuristics. Fig. 6 shows that the analytical approach diverges considerably beyond 0.7 seconds, and that reducing the size of the latent space to  $64 \times 32 \times 32$  improves inference time by 30% but yields larger errors.

TABLE III: Comparison on internal dataset at 3 seconds horizon.

Model	Metric	ADE (m)	FDE (m)
analytical baseline		1.10	2.65
PredictionNet (ours)		<b>0.62</b>	<b>1.36</b>

## B. Real-world Autonomous Driving

We integrated our PredictionNet system into an actuated real-world vehicle. We use the DNN to predict 3 seconds into the future, and then extrapolate the result from 3 to 5 seconds using the analytical predictor. We chose this combination as a trade-off between accuracy and performance: the DNN reacts to important events within the 3 second horizon, while analytical extrapolation reduces run-time latency.

To quantify performance, we assume that better prediction leads to better planning and hence more driving comfort by avoiding harsh braking or emergency disengagements. Each route is split into segments of a few seconds each, and the average jerk (derivative of acceleration) is computed for each segment. We classify segments as “comfortable” or “not comfortable” based on a threshold from trials with human drivers. The final score is the percentage of route segments that are “comfortable”.

This system was used for actuated drives on routes in Washington state and California for approximately 530 km in total. The network consumes perception output from cameras and radars, even though it was trained on LiDAR-derived data. We encountered no network-related safety disengagements. The DNN was able to handle non-mapped areas in the real world thanks to a training procedure that includes random map dropouts. Compared to the analytic baseline, PredictionNet improved the mean comfort score by **15%** and reduced standard deviation by **18%**.

PredictionNet is also extremely computationally efficient. The DNN inference time is around **5 ms** and the pre-/post-processing time is **3 ms** on an embedded NVIDIA’s Drive AGX computer. To our knowledge, our system is the fastest DNN-based approach available for real-world traffic prediction.

## C. Simulation Performance

To measure the adequacy of PredictionNet for simulation, we used it as an environment step function of a standard OpenAI Gym environment [39]. We used our large internal dataset containing dense multi-agent interactions to sample initial traffic states. To measure performance, we focused on collision rates and off-route driving rates, which were computed using the environment’s contact detectors and the lane geometry (to determine non-drivable areas), respectively.

Table IV shows the simulation failure rates among all environment steps for both PredictionNet and an analytical baseline. Log-replay is applied for 1.33 seconds, then all vehicles are controlled for an additional 6.67 seconds by either PredictionNet or the unicycle model [34], the latter of which is applied to vehicle kinematics while maintaining constant heading and speed. Total episode length is 8.0 seconds. Failure is declared when the vehicle leaves the drivable area (“off-road”) or intersects another vehicle (“collision”). Furthermore, for “reactive collision” we apply harsh braking to random agents. We observe that PredictionNet reliably avoids collisions and remains in the drivable area. Our approach outperforms the baseline on all metrics by a large margin.

TABLE IV: Simulation comparison, showing the percentage of failures over all environment steps.

Model \ Metric	off-road	collision	reactive collision
baseline	2.1%	8.7%	7.1%
PredictionNet	<b>1.4%</b>	<b>4.1%</b>	<b>5.3%</b>

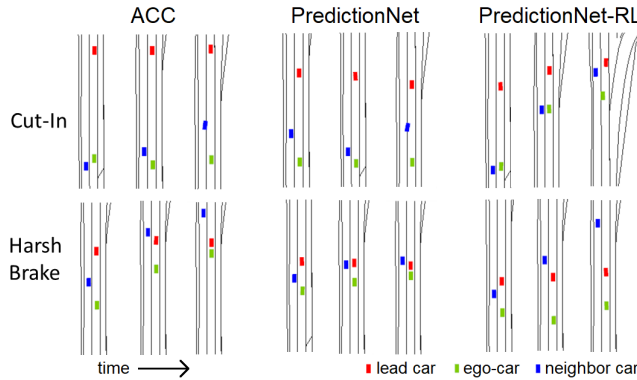


Fig. 7: PredictionNet-RL outperforms both PredictionNet and ACC for the cut-in and harsh braking scenarios. Shown are 3 time slices from left to right for each policy.

#### D. Ego-Policy Performance

We use reinforcement learning (RL) to improve handling of rare and unsafe events like cut-ins and harsh-braking. We aim to improve upon both traditional adaptive cruise control (ACC) and imitation learning-based driving policies. Our PredictionNet-RL uses the Soft Actor Critic algorithm (SAC) [40] to train the policy and critic heads, while keeping PredictionNet trunk weights frozen. The latent vector  $s_t = h_t$  is fed into three fully convolutional layers to extract features, and each of the policy and critic heads is a three-layer MLP. The MDP discount factor is  $\gamma = 0.95$ . The ACC reward function is  $r_{acc} = \alpha_1|\Delta_a| + \alpha_2|\Delta_v| + \alpha_3d$  where  $\Delta_a, \Delta_v$  denote the changes in acceleration and velocity, and  $d$  denotes the distance to the lead car;  $\alpha_{1,2,3}$  are tuned to accomplish smooth following in real-world scenarios. We use episodes with randomized initial conditions. An episode ends if a collision or cut-in happens with task-specific penalty  $r_{rare} = -1$ , or reaches the maximum number (48) of episode steps. We generate and detect cut-ins or braking signals based on agents' headings and accelerations.

We evaluate our learned policies in separate cut-in and harsh-braking tasks. We compare PredictionNet-RL policy with vanilla PredictionNet ego-prediction that only captures expert driving via supervised learning. We also compare with an internal implementation of ACC. In Table V, we test each policy with 10 different runs, observing that PredictionNet-RL reaches the best performance for both tasks.

Fig. 7 shows some qualitative results. In the cut-in scenarios, the neighbor car (blue) attempts to cut in between the lead car (red) and ego car (green). Whereas both ACC and vanilla PredictionNet allow this cut-in, PredictionNet-RL learns to speed up to prevent these aggressive cut-in maneuvers. In the harsh braking case, the lead car (red) performs sudden braking. Whereas both ACC and PredictionNet cause the ego car to come dangerously close to the

TABLE V: Policy learning comparison, showing the percentage of failures for 10 test episodes.

Task \ Policy	ACC	PredictionNet	PredictionNet-RL
Cut-In	88%	56%	<b>2%</b>
Harsh Brake	100%	60%	<b>0%</b>

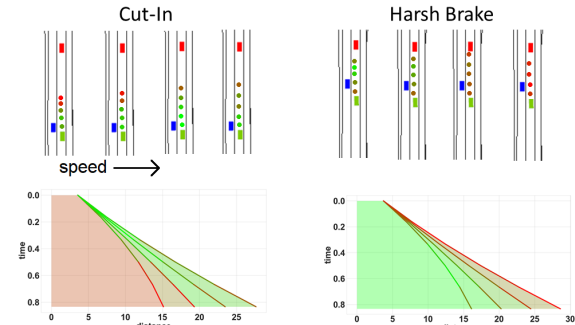


Fig. 8: Visualization of the RL value function for 4 speed profiles for each of the two tasks. TOP: Top-down view, with circles denoting sampled states colored by the value function. BOTTOM: Value function computed along 4 speed profiles. The  $y$ -axis denotes the time horizon, while  $x$ -axis denotes the distance from the state  $s_{t+1}$ . Each trajectory curve is colored according to the value function, with green denoting higher critic rewards, and red denoting lower rewards. The space between speed profile curves is filled with the average nearby color.

lead car, the PredictionNet-RL agent learns to slow down to avoid collision with the lead car. Overall, such sparse-reward scenarios are challenging for the baselines since the rare events are underrepresented in the training data.

Fig. 8 visualizes the learned RL value function [41] for 4 possible speed profiles for each of the two tasks, together with sampled top-down time-steps. As traffic speed increases, the ego-vehicle is rewarded for speeding up to discourage cut-in, and for braking quickly to avoid collision.

## V. CONCLUSION

In this work, we presented PredictionNet, a real-time DNN for trajectory prediction that can efficiently forecast trajectories of all traffic actors simultaneously. We showed that a well-trained prediction system provides an efficient data-driven traffic simulator that significantly outperforms heuristic-based baselines. Furthermore, our experiments with an RL-based extension show significant improvement for rare events that are not captured in the expert dataset. We validated our approach in simulation, on off-line datasets, and via on-line real-world actuated driving. For future work, we plan to incorporate the direct trajectory regression into the network, use live map perception, and transfer our RL experiments to the real vehicle.

## ACKNOWLEDGMENT

We would like to acknowledge Rotem Aviv and Ruchi Bhargava for support. We thank Fangkai Yang and Ryan Oldja for system work.

## REFERENCES

[1] W. Yoshida, R. J. Dolan, and K. J. Friston, “Game theory of mind,” *PLoS computational biology*, vol. 4, no. 12, 2008.

[2] P. Hernandez-Leal, B. Kartal, and M. E. Taylor, “Agent modeling as auxiliary task for deep reinforcement learning,” in *Proceedings of the AAAI Conference on Artificial Intelligence and Interactive Digital Entertainment*, vol. 15, no. 1, 2019, pp. 31–37.

[3] N. Lee, W. Choi, P. Vernaza, C. B. Choy, P. H. Torr, and M. Chandraker, “DESIRE: Distant future prediction in dynamic scenes with interacting agents,” in *Proceedings of the IEEE Conference on Computer Vision and Pattern Recognition*, 2017, pp. 336–345.

[4] N. Rhinehart, R. McAllister, K. Kitani, and S. Levine, “PRECOOG: PREdiction conditioned on goals in visual multi-agent settings,” in *Proceedings of the IEEE/CVF International Conference on Computer Vision*, 2019, pp. 2821–2830.

[5] Y. Chai, B. Sapp, M. Bansal, and D. Anguelov, “MultiPath: Multiple probabilistic anchor trajectory hypotheses for behavior prediction,” in *CoRL*, 2019.

[6] N. Djuric, H. Cui, Z. Su, S. Wu, H. Wang, F.-C. Chou, L. S. Martin, S. Feng, R. Hu, Y. Xu, et al., “MultiXNet: Multiclass multistage multimodal motion prediction,” in *IEEE Intelligent Vehicles Symposium*, 2020.

[7] S. Casas, C. Gulino, S. Suo, K. Luo, R. Liao, and R. Urtasun, “Implicit latent variable model for scene-consistent motion forecasting,” in *ECCV*, 2020, pp. 624–641.

[8] T. Salzmann, B. Ivanovic, P. Chakravarty, and M. Pavone, “Trajectron++: Dynamically-feasible trajectory forecasting with heterogeneous data,” in *ECCV*, 2020, pp. 683–700.

[9] W. Zhan, L. Sun, D. Wang, H. Shi, A. Clausse, M. Naumann, J. Kummerle, H. Konigshof, C. Stiller, A. de La Fortelle, et al., “Interaction dataset: An international, adversarial and cooperative motion dataset in interactive driving scenarios with semantic maps,” *arXiv preprint arXiv:1910.03088*, 2019.

[10] D. P. Kingma and M. Welling, “Auto-encoding variational bayes,” *arXiv preprint arXiv:1312.6114*, 2013.

[11] J. Gao, C. Sun, H. Zhao, Y. Shen, D. Anguelov, C. Li, and C. Schmid, “VectorNet: Encoding HD maps and agent dynamics from vectorized representation,” in *Proceedings of the IEEE/CVF Conference on Computer Vision and Pattern Recognition (CVPR)*, 2020.

[12] Z. Wu, S. Pan, F. Chen, G. Long, C. Zhang, and S. Y. Philip, “A comprehensive survey on graph neural networks,” *IEEE transactions on neural networks and learning systems*, vol. 32, no. 1, pp. 4–24, 2020.

[13] A. Dosovitskiy, G. Ros, F. Codevilla, A. Lopez, and V. Koltun, “CARLA: An open urban driving simulator,” in *Conference on robot learning (CoRL)*, 2017.

[14] P. A. Lopez, M. Behrisch, L. Bieker-Walz, J. Erdmann, Y.-P. Flötteröd, R. Hilbrich, L. Lücken, J. Rummel, P. Wagner, and E. Wießner, “Microscopic traffic simulation using sumo,” in *International Conference on Intelligent Transportation Systems (ITSC)*, 2018, pp. 2575–2582.

[15] S. Suo, S. Regaldo, S. Casas, and R. Urtasun, “TrafficSim: Learning to simulate realistic multi-agent behaviors,” in *Proceedings of the IEEE/CVF Conference on Computer Vision and Pattern Recognition (CVPR)*, 2021.

[16] L. Bergamini, Y. Ye, O. Scheel, L. Chen, C. Hu, L. Del Pero, B. Osinski, H. Grimmett, and P. Ondruska, “SimNet: Learning reactive self-driving simulations from real-world observations,” in *ICRA*, 2021.

[17] M. Buehler, K. Iagnemma, and S. Singh, *The DARPA Urban Challenge: Autonomous Vehicles in City Traffic*. Springer, 2009, vol. 56.

[18] H. Fan, F. Zhu, C. Liu, L. Zhang, L. Zhuang, D. Li, W. Zhu, J. Hu, H. Li, and Q. Kong, “Baidu Apollo EM motion planner,” in *arXiv:1807.08048*, 2018.

[19] W. Zeng, W. Luo, S. Suo, A. Sadat, B. Yang, S. Casas, and R. Urtasun, “End-to-end interpretable neural motion planner,” in *Proceedings of the IEEE/CVF Conference on Computer Vision and Pattern Recognition*, 2019, pp. 8660–8669.

[20] A. Sadat, M. Ren, A. Pokrovsky, Y.-C. Lin, E. Yumer, and R. Urtasun, “Jointly learnable behavior and trajectory planning for self-driving vehicles,” in *IEEE/RSJ International Conference on Intelligent Robots and Systems (IROS)*, 2019, pp. 3949–3956.

[21] M. Henaff, A. Canziani, and Y. LeCun, “Model-predictive policy learning with uncertainty regularization for driving in dense traffic,” in *ICLR*, 2019.

[22] D. A. Pomerleau, “ALVINN: An autonomous land vehicle in a neural network,” in *Proceedings of Neural Information Processing Systems (NeurIPS)*, 1989.

[23] N. D. Ratliff, J. A. Bagnell, and M. A. Zinkevich, “Maximum margin planning,” in *Proceedings of the 23rd International Conference on Machine Learning (ICML)*, 2006, pp. 729–736.

[24] M. Bansal, A. Krizhevsky, and A. Ogale, “ChauffeurNet: Learning to drive by imitating the best and synthesizing the worst,” in *Robotics Science and Systems (RSS)*, 2019.

[25] F. Codevilla, M. Müller, A. López, V. Koltun, and A. Dosovitskiy, “End-to-end driving via conditional imitation learning,” in *IEEE International Conference on Robotics and Automation (ICRA)*, 2018, pp. 4693–4700.

[26] S. Ross, G. Gordon, and D. Bagnell, “A reduction of imitation learning and structured prediction to no-regret online learning,” in *Proceedings of the Fourteenth International Conference on Artificial Intelligence and Statistics*, 2011, pp. 627–635.

[27] P. Wolf, C. Hubschneider, M. Weber, A. Bauer, J. Härtl, F. Dürr, and J. M. Zöllner, “Learning how to drive in a real world simulation with deep q-networks,” in *IEEE Intelligent Vehicles Symposium (IV)*, 2017, pp. 244–250.

[28] B. R. Kiran, I. Sobh, V. Talpaert, P. Mannion, A. A. Al Sallab, S. Yoganani, and P. Pérez, “Deep reinforcement learning for autonomous driving: A survey,” *IEEE Transactions on Intelligent Transportation Systems*, 2021.

[29] S. Shalev-Shwartz, S. Shammah, and A. Shashua, “Safe, multi-agent, reinforcement learning for autonomous driving,” in *NeurIPS workshop*, 2016.

[30] T. P. Lillicrap, J. J. Hunt, A. Pritzel, N. Heess, T. Erez, Y. Tassa, D. Silver, and D. Wierstra, “Continuous control with deep reinforcement learning,” in *ICLR*, 2015.

[31] J. Chen, B. Yuan, and M. Tomizuka, “Model-free deep reinforcement learning for urban autonomous driving,” in *IEEE Intelligent Transportation Systems Conference (ITSC)*, 2019, pp. 2765–2771.

[32] D. M. Saxena, S. Bae, A. Nakhaei, K. Fujimura, and M. Likhachev, “Driving in dense traffic with model-free reinforcement learning,” in *IEEE International Conference on Robotics and Automation (ICRA)*, 2020, pp. 5385–5392.

[33] T.-Y. Lin, P. Goyal, R. B. Girshick, K. He, and P. Dollar, “Focal loss for dense object detection,” in *ICCV*, 2017.

[34] S. M. LaValle, *Planning algorithms*. Cambridge University Press, 2006.

[35] L. Chen, G. Papandreou, I. Kokkinos, K. Murphy, and A. L. Yuille, “DeepLab: Semantic image segmentation with deep convolutional nets, atrous convolution, and fully connected crfs,” *IEEE Transactions on Pattern Analysis and Machine Intelligence (PAMI)*, vol. 40, no. 4, Apr. 2018.

[36] H. Zhao, J. Gao, T. Lan, C. Sun, B. Sapp, B. Varadarajan, Y. Shen, Y. Shen, Y. Chai, C. Schmid, C. Li, and D. Anguelov, “TNT: target-driven trajectory prediction,” in *arXiv:2008.08294*, 2020.

[37] X. Mo, Y. Xing, and C. Lv, “ReCoG: A deep learning framework with heterogeneous graph for interaction-aware trajectory prediction,” in *arXiv:2012.05032*, 2021.

[38] A. Scibior, V. Lioutas, D. Reda, P. Bateni, and F. Wood, “Imagining the road ahead: Multi-agent trajectory prediction via differentiable simulation,” in *IEEE International Conference on Intelligent Transportation Systems (ITSC)*, 2021.

[39] G. Brockman, V. Cheung, L. Pettersson, J. Schneider, J. Schulman, J. Tang, and W. Zaremba, “OpenAI gym,” *arXiv preprint arXiv:1606.01540*, 2016.

[40] T. Haarnoja, A. Zhou, P. Abbeel, and S. Levine, “Soft actor-critic: Off-policy maximum entropy deep reinforcement learning with a stochastic actor,” in *International Conference on Machine Learning (ICML)*, 2018, pp. 1861–1870.

[41] R. S. Sutton and A. G. Barto, *Reinforcement Learning: An Introduction*, 2nd ed. The MIT Press, 2018.